Inorganic Chemistry
Article

Inorg. Chem. **2010**, *49*, 2773–2781 **2773**
DOI: 10.1021/ic902151d

Ruthenium Intermetallics Grown from La−Ni Flux: Synthesis, Structure, and Physical Properties

Julia V. Zaikina,[†] Young-Jung Jo,[‡] and Susan E. Latturner*,[†]

[†]*Department of Chemistry and Biochemistry, Florida State University, Tallahassee, Florida 32306, and* [‡]*Applied Superconductivity Center, National High Magnetic Field Laboratory, Tallahassee, Florida 32310*

Received November 2, 2009

Crystals of three new intermetallic compounds were grown from reactions of ruthenium with other elements in $La_{0.8}Ni_{0.2}$ eutectic flux. The new boride $LaRu_2Al_2B$ crystallizes in a filled $CeMg_2Si_2$ structure type (*P*4/*mmm*, *a* = 4.2105(5) Å, *c* = 5.6613(8); *Z* = 1, R_1 = 0.014), with Ru atoms forming a planar square net; B atoms center alternating Ru squares, which is an unusual coordination of boron by transition metals. Al atoms connect the Ru_2B layers, forming large voids where La ions reside. The chemical bonding analysis using the electron localization function (ELF) reveals two-center covalent bonding between Al atoms, an absence of direct Ru−Ru interactions, and three-centered bonds between Ru and B or Al atoms. The band structure calculation shows $LaRu_2Al_2B$ to be metallic, which is in agreement with the observed temperature independent paramagnetism and heat capacity data. The crystal structure of $La_2Ni_{2-x}Ru_xAl$ (HT-Pr_2Co_2Al-type; *x* = 0.21(1) and *x* = 0.76(1); *C*2/*c*; *a* = 9.9001(3) Å, *b* = 5.7353(1) Å, *c* = 7.8452(2) Å, β = 104.275(1); *Z* = 4, R_1 = 0.016 for *x* = 0.76(1)) features infinite $[Ni_{2-x}Ru_xAl]$ spiral-twisted chains composed of Al_2M_2-rhombic units (M = Ni/Ru) seen in many La−Ni−Al intermetallics. The structure of $La_6SnNi_{3.67}Ru_{0.76}Al_{3.6}$ ($Nd_6Co_5Ge_{2.2}$-type; $P\bar{6}m2$, *a* = 9.620(1) Å, *c* = 4.2767(9) Å; *Z* = 1, R_1 = 0.015) is composed of a three-dimensional $[Ni_{3.67}Ru_{0.76}Al_{3.6}]^3{}_\infty$ network with large hexagonal channels accommodating interconnected tin-centered lanthanum clusters Sn@La_9.

Introduction

Synthesis in molten metal solvents (flux growth) has proven to be an effective method to obtain high-quality single crystals of intermetallic compounds, including phases which are incongruently melting or metastable.[1] Flux reactions facilitate exploratory synthesis,[2] often leading to discovery of new compounds with complex crystal structures and/or odd stoichiometries. Useful fluxes can range from low-melting elements such as Ga, Sn, Al, In, and Pb, to more esoteric eutectic mixtures of metals.[1] Lanthanum and nickel are not considered useful fluxes because of their high melting points. However, when combined in a 88/12 wt % ratio, these metals form a low-melting eutectic.[3] The use of La/Ni eutectic as a flux was recently shown to be an attractive synthesis technique which leads to the formation of new phases, for example, $La_{21}Fe_8E_7C_{12}$ (E = Bi, Sn, Sb, Te, Ge)[4] and allows the growth of large crystals of peritectic phases such as $La_6T_{13-x}Al_xM_y$ (T = Mn, Fe; M = main group element).[5]

La/Ni flux is composed of a highly reactive metal (lanthanum) together with a more inert component (nickel). Reactions of iron in this flux predominantly yield La/Fe/X phases, with no nickel incorporation. Syntheses with ruthenium were carried out to determine if this trend would also be seen with iron's heavier congener. Another interesting aspect of two-component flux systems is their ability to dissolve normally intractable elements. Carbon readily dissolves in La/Ni flux, and we are now finding that the solubilizing effect can be extended to boron.

The outstanding properties of borides have been extensively investigated for more than 50 years, with widespread interest sparked by discovery of superconductivity in MgB_2. Intermetallic borides have attracted substantial attention because of their hardness and oxidation resistance.[6]

*To whom correspondence should be addressed. E-mail: latturne@chem.fsu.edu. Phone: (850) 644-4074. Fax: (850) 644-8281.

(1) (a) Kanatzidis, M. G.; Pöttgen, R.; Jeitschko, W. *Angew. Chem., Int. Ed.* **2005**, *44*, 6996–7023. (b) P. C. Canfield, P. C.; Fisher, I. R. *J. Cryst. Growth* **2001**, *225*, 155–161.

(2) (a) Corbett, J. D. *Inorg. Chem.* **2000**, *39*, 5178–5191. (b) Corbett, J. D. *Inorg. Chem.* **2010**, *49*, 13–28.

(3) Massalski, T. B.; Okamoto, H. *Binary Alloy Phase Diagrams*, 2nd ed.; ASM International: Materials Park, OH, 1990.

(4) Benbow, E. M.; Dalal, N. S.; Latturner, S. E. *J. Am. Chem. Soc.* **2009**, *131*(9), 3349–3354.

(5) Benbow, E. M.; Dalal, N. S.; Latturner, S. E. *J. Solid State Chem.* **2009**, *182*, 3055–3062.

(6) (a) Levine, J. B.; Nguyen, S. L.; Rasool, H. I.; Wright, J. A.; Brown, S. E.; Kaner, R. B. *J. Am. Chem. Soc.* **2008**, *130*, 16953–16958. (b) Weinberger, M. B.; Levine, J. B.; Chung, H. Y.; Cumberland, R. W.; Rasool, H. I.; Yang, J. M.; Kaner, R. B.; Tolbert, S. H. *Chem. Mater.* **2009**, *21*, 1915–1921. (c) Sciti, D.; Silvestroni, L.; Celotti, G.; Melandri, C.; Guicciardi, S. *J. Am. Ceram. Soc.* **2008**, *91*, 3285–3291. (d) Post, B.; Glaser, F. W. *Refractory Binary Borides*; Interscience: New York, 1963.

Published on Web 02/08/2010

Borides of transition metals exhibit a diversity of crystal structure types and a variety of interesting physical properties, including itinerant magnetism, superconductivity, heavy-fermion behavior, and valence fluctuations.[7−10] The common synthesis method for borides is arc-melting followed by long-term annealing with intermediate grinding; however, large single crystals of borides have been accessed via growth in Al, Cu, and Li fluxes.[1] In the course of our exploratory synthesis aiming to produce new borides of ruthenium, we discovered three new compounds $LaRu_2Al_2B$, $La_2Ni_{2-x}Ru_xAl$, and $La_6SnNi_{3.67}Ru_{0.76}Al_{3.6}$. In this work we discuss their synthesis and crystal structures, as well as the electronic and physical properties of $LaRu_2Al_2B$.

Experimental Procedure

Sample Preparation. Preparation, handling, and storage of the starting materials and products were carried out in an argon-filled glovebox. Powders of lanthanum (99.9%, Metall Rare Earth Ltd., ∼60 mesh), ruthenium (99.9%, ∼325 mesh, Alfa Aesar), aluminum (99%, Strem Chemicals), amorphous boron (95−97%, Strem Chemicals), tin (99.9%, ∼20 mesh, Fisher Chemicals) and ingots of La−Ni eutectic (88:12 wt %, Alfa Aesar, 99.9%) were used as received. The synthesis technique is analogous to that of $La_{21}Fe_8Sn_7C_{12}$.[4] La, Ru, Sn, and B reactants, mixed in 1:1:1:1 molar ratio (total mass 0.35 g), were sandwiched between layers of La/Ni eutectic (∼1.2 g) in an alumina crucible (ID 6 mm), which was placed in a silica tube. A second alumina crucible was filled with Fiberfrax and inverted above the reaction crucible to act as a filter during centrifugation. The silica tube was fused under vacuum of 10^{-2} Torr; the ampule was then heated to 1000 °C in 3 h, held at this temperature for 12 h, and then cooled to 850 °C in 10 h. The reaction mixture was subsequently annealed for 48 h at 850 °C and then cooled to 600 °C in 84 h. At 600 °C the ampule was removed from the furnace, quickly inverted, and placed into a centrifuge for decanting of the molten flux. Flux remaining on the surface of the product can be removed by briefly leaving the crystals in air to preferentially oxidize the La-rich flux coating. Products were then kept in a glovebox to prevent further oxidation. Crystals of $LaRu_2Al_2B$ (I), $La_2Ni_{1.79(1)}Ru_{0.21(1)}Al$ (II) and $La_6SnNi_{3.67}Ru_{0.76}Al_{3.6}$ (IV) were isolated from this sample. Crystals of $La_2Ni_{1.24(1)}Ru_{0.76(1)}Al$ (III) were obtained from another reaction with starting composition of La:Ru:Sn:C in a 1:1:1:1 molar ratio. Aluminum was leached from the alumina crucible. The $LaRu_2Al_2B$ phase was subsequently synthesized in higher yield from reaction of La, Ru, Al, B mixed in 1:2:2:1 molar ratio (total mass 0.5 g) layered between La/Ni eutectic (∼1.2 g), the only differences being the deliberate addition of aluminum and absence of tin, as well as the higher centrifugation temperature of 650 °C.

Elemental Analysis. Semiquantitative elemental analysis was performed with energy-dispersive X-ray spectroscopy (EDXS) on a JEOL 5900 scanning electron microscope equipped with PGT Prism energy dispersion spectroscopy software. Crystals were mounted onto an aluminum holder using double-sided carbon tape, oriented with a flat face perpendicular to the beam and analyzed using a 30 kV accelerating voltage and an accumulation time of 60 s. The boron content was not determined because of the limitation of EDXS with light elements.

Single Crystal X-ray Diffraction Experiments and Structure Determination. Selected single crystals were mounted on glass fibers using epoxy. The X-ray intensity data were collected at room temperature on a Bruker SMART APEX2 CCD diffractometer equipped with a MoKα X-ray tube (λ = 0.71073 Å). The detector was placed at a distance of 6 cm from the crystal. A total of 2400 frames were collected with a scan width of 0.3° in ω and an exposure time of 20 s/frame for low-angle area and 30 s/frame for high-angle regions. The frames were integrated with the Bruker SAINT software package[11] using a narrow-frame integration algorithm to a maximum 2θ angle of 56°−75°. Data were corrected for absorption effects using the empirical method (SADABS[12]). The structures were solved and refined by full-matrix least-squares procedures on $|F^2|$ using the SHELX-97 software package.[13a]

$LaRu_2Al_2B$ (I). The highest symmetry space group $P4/mmm$ (no. 123) was chosen for the structure solution. The occupancies for all atom positions were allowed to vary but refined close to unity.

$La_2Ni_{2-x}Ru_xAl$ (x = 0.21(2) (II) and 0.76(1) (III)). The crystal structure solutions were performed in the centrosymmetric space group $C2/c$ (no. 15). The refinements showed occupancy higher than 100% at position 8*f* when assigned as Ni. On the basis of composition from EDXS, this position was set as mixed occupied by nickel and ruthenium atoms.

$La_6SnNi_{3.67}Ru_{0.76}Al_{3.6}$ (IV). The structure was solved in noncentrosymmetric group $P\bar{6}m2$ (no. 187) (R_{int} = 0.028). Further refinement showed that the Flack parameter is equal to 0.54, which may indicate racemic twinning. The refinement of the twin ratio (using the BASF command in SHELXL) led to a value of 0.57. Refinement of occupancies showed that all positions are fully occupied except for 1*a* and 3*j*. EDXS analysis of the crystal used for data collection, and of several other crystals with the same unit cell, indicate a consistent La/Sn/Ru ratio of 6:1:0.5. On the basis of this, the position 3*j* was refined as jointly occupied by Ni/Ru, while position 1*a* was refined as Ru/Al. However, the possibility of mixed occupancy of these sites by three atoms, for example, Ru/Ni/Al, cannot be excluded. The structure solution was checked with the program Platon[13b] and no higher symmetry was found.

The final refinements with anisotropic atomic displacement parameters (ADP) for all atoms converged to R_1 = 0.014, 0.027, 0.016, and 0.015 leading to the compositions $LaRu_2Al_2B$ (I), $La_2Ni_{1.79(1)}Ru_{0.21(1)}Al$ (II), $La_2Ni_{1.24(1)}Ru_{0.76(1)}Al$ (III), and $La_6SnNi_{3.67(3)}Ru_{0.76(4)}Al_{3.572(7)}$ (IV), respectively. The details of the data collection and refinement are summarized in Table 1, the atomic positions are given in Table 2, and selected bond distances are listed in Table 3.

Magnetic Properties. The magnetic susceptibility of $LaRu_2Al_2B$ was measured over the temperature range 1.8−300 K in external magnetic fields from 10 to 3000 Oe using a SQUID magnetometer (Quantum Design MPMS system). The powder, prepared by grinding single crystals in the glovebox, was contained

(7) Mori, T. In *Handbook on the Physics and Chemistry of Rare-Earths*; Gschneidner, K. A., Jr., Bunzli, J.-C., Pecharsky, V., Eds.; North-Holland: Amsterdam, 2008; Vol. *38*.

(8) (a) Dronskowski, R.; Korczak, K.; Lueken, H.; Jung, W. *Angew. Chem., Int. Ed.* **2002**, *41*(14), 2528–2532. (b) Fokwa, B. P. T.; Samolyuk, G. D.; Miller, G. J.; Dronskowski, R. *Inorg. Chem.* **2008**, *47*, 2113–2120. (c) Dhar, S. K.; Malik, S. K.; Vijayaraghavan, R. *J. Phys. C: Solid State Phys.* **1981**, *14*, L321–L324.

(9) (a) Klimczuk, T.; Xu, Q.; Morosan, E.; Thompson, J. D.; Zandbergen, H. W.; Cava, R. J. *Phys. Rev. B* **2006**, *74*, 220502. (b) Fertig, W. A.; Johnston, D. C.; Delong, L. E.; Mccalum, R. W.; Maple, M. B. *Phys. Rev. Lett.* **1977**, *38* (17), 987–990. (c) Athreya, K. S.; Hausermann-Berg, L. S.; Shelton, R. N.; Malik, S. K.; Umarji, A. M.; Shenoy, G. K. *Phys. Lett. A* **1985**, *113A*(6), 330–334. (d) Maple, M. B.; Lambert, S. E.; Torikachvili, M. S.; Yang, K. N.; Allen, J. W.; Pate, B. B.; Lindau, I. *J. Less-Comm. Met.* **1985**, *111*, 239–249. (e) Fujimori, A.; Takahashi, T.; Okabe, A.; Kasaya, M.; Kasuya, T. *Phys. Rev. B* **1990**, *41*, 6783–6787.

(10) Kuzma, Yu.B. *Crystal Chemistry of Borides*; Vyscha Shkola: Lviv, 1983.

(11) *SAINT*; Bruker AXS Inc.: Madison, WI, 2008.

(12) *SADABS*; Bruker AXS Inc.: Madison, WI, 2008.

(13) (a) Sheldrick, G. M. *Acta Crystallogr.* **2008**, *A64*, 112–122. (b) Spek, A. L. *Acta Cryst. A* **1990**, *46*, C34.

Table 1. Data Collection and Structure Refinement Parameters for $LaRu_2Al_2B$ (I), $La_2Ni_{1.79(1)}Ru_{0.21(1)}Al$ (II), $La_2Ni_{1.24(1)}Ru_{0.76(1)}Al$ (III), and $La_6SnNi_{3.67}Ru_{0.76}Al_{3.6}$ (IV)[a]

	$LaRu_2Al_2B$ (I)	$La_2Ni_{1.79(1)}Ru_{0.21(1)}Al$ (II)	$La_2Ni_{1.24(1)}Ru_{0.76(1)}Al$ (III)	$La_6SnNi_{3.67(3)}Ru_{0.76(4)}Al_{3.572(7)}$ (IV)
crystal system	tetragonal	monoclinic	monoclinic	hexagonal
space group	*P*4/*mmm* (no. 123)	*C*2/*c* (no. 15)	*C*2/*c* (no. 15)	$P\bar{6}m2$ (no 187)
collection temperature, K	298(2)	298(2)	298(2)	298(2)
cell parameters				
a/Å	4.2105(5)	9.782(1)	9.9001(3)	9.620(1)
b/Å		5.6840(7)	5.7353(1)	
c/Å	5.6613(8)	7.940(1)	7.8452(2)	4.2767(9)
β		104.339(1)°	104.275(1)°	
V, Å^3	100.37(2)	427.70(9)	431.70(2)	342.78(9)
Z	1	4	4	1
density (calc) [g cm^{-3}]	6.71	6.70	7.00	6.50
extinction coef.	0.234(9)	0.0005(1)	0.0034(2)	0.0047(3)
μ, [mm^{-1}]	18.1	28.0	27.3	25.9
data collection range, deg.	$3.60 < \theta < 37.72$	$4.18 < \theta < 26.99$	$4.14 < \theta < 32.47$	$2.44 < \theta < 34.01$
reflections collected	1402	1771	2371	4685
independent reflections	191 [$R_{int} = 0.012$]	461 [$R_{int} = 0.026$]	706 [$R_{int} = 0.017$]	574 [$R_{int} = 0.016$]
parameters refined	12	26	26	27
R_1[b]	0.014	0.020	0.015	0.015
wR_2[c] [$F_o > 4\sigma F_o$]	0.036	0.041	0.036	0.030
R_1, wR_2 (all data)	0.014, 0.036	0.027, 0.043	0.016, 0.036	0.015, 0.030
largest diff. peak and hole [e/Å^3]	1.13 and −2.36	0.94 and −0.79	0.95 and −0.84	1.24 and −0.90
goodness-of-fit	1.185	0.988	1.055	1.228

[a] Further details of the crystal structure determination may be obtained from Fachinformationszentrum Karlsruhe, D-76344 Eggenstein-Leopoldshafen, Germany, on quoting the depository numbers CSD-421103, CSD-421100, CSD-421101, and CSD-421102 for I, II, III, and IV, respectively. [b] $R_1 = \sum||F_o| - |F_c||/\sum|F_o|$. [c] $wR_2 = [\sum w(F_o^2 - F_c^2)^2/\sum w(F_o^2)^2]^{1/2}$, $w = [\sum^2(F_o^2) + (Ap)^2 + Bp]^{-1}$; $p = (F_o^2 + 2F_c^2)/3$; $A = 0.0226$ (I), 0.022800 (II), 0.0184 (III), 0.0086 (IV); $B = 0.057$ (I), 0 (II), 1.0507 (III), 0.5619 (IV).

Table 2. Atomic Coordinates, Site Occupancy Factors (s.o.f.), and Thermal Displacement Parameters for $LaRu_2Al_2B$ (I), $La_2Ni_{1.79(1)}Ru_{0.21(1)}Al$ (II), $La_2Ni_{1.24(1)}Ru_{0.76(1)}Al$ (III), and $La_6SnNi_{3.67}Ru_{0.76}Al_{3.6}$ (IV)

Atom	Wyckoff	*x*/*a*	*y*/*b*	*z*/*c*	s.o.f.	U_{eq}[a]
			$LaRu_2Al_2B$			
La(1)	1*b*	0	0	1/2	1	0.0064(1)
B(2)	1*a*	0	0	0	1	0.0069(9)
Ru(3)	2*f*	0	1/2	0	1	0.0046(1)
Al(4)	2*h*	1/2	1/2	0.2537(2)	1	0.0066(2)
			$La_2Ni_{1.8}Ru_{0.2}Al$			
La(1)	8*f*	0.35191(4)	0.14394(6)	0.35213(4)	1	0.0127(1)
Ni(2)/Ru(2)	8*f*	0.13271(8)	0.1347(1)	0.00436(9)	0.892(6)/ 0.108	0.0160(3)
Al(3)	4*e*	0	0.1306(4)	1/4	1	0.0106(5)
			$La_2Ni_{1.2}Ru_{0.8}Al$			
La(1)	8*f*	0.35243(2)	0.14093(3)	0.35219(2)	1	0.01214(6)
Ni(2)/Ru(2)	8*f*	0.13431(4)	0.13686(5)	0.00719(4)	0.619(5)/ 0.381	0.0164(1)
Al(3)	4*e*	0	0.1222(2)	1/4	1	0.0115(2)
			$La_6SnNi_{3.67}Ru_{0.76}Al_{3.6}$			
La(1)	3*k*	0.87215(2)	0.12785(2)	1/2	1	0.01488(9)
La(2)	3*j*	0.50892(2)	0.49108(2)	0	1	0.01203(9)
Ni(3)/Ru(3)	3*j*	0.15244(5)	0.84756(5)	0	0.89(1)/0.11	0.0150(3)
Al(4)	3*k*	0.2371(1)	0.7629(1)	1/2	1	0.0115(4)
Sn(5)	1*f*	2/3	1/3	1/2	1	0.0132(2)
Ni(6)	1*c*	1/3	2/3	0	1	0.0143(3)
Al(7)/Ru(7)	1*a*	0	0	0	0.572(7)/0.428	0.022(6)

[a] U_{eq} is defined as one-third of the trace of the orthogonalized U_{ij} tensor.

in a gelatin capsule inserted in a plastic straw. The susceptibility was corrected for contributions from the holder and underlying sample diamagnetism.

Heat Capacity. A plate-like crystal of $LaRu_2Al_2B$ (largest dimension of 1 mm, mass = 2.18 mg) was used to measure heat capacity. The heat capacity measurement was performed on a Quantum Design Physical Property Measurement System (PPMS) in zero-field at temperatures between 2 and 100 K.

Quantum Chemical Calculations. Calculations of band structure, density of states (DOS), and electron localization function (ELF) were performed with the tight binding-linear muffin tin orbitals-atomic sphere approximation TB-LMTO-ASA program package, based on the experimentally determined unit cell dimensions and atomic coordinates for $LaRu_2Al_2B$.[14a] The radial scalar-relativistic Dirac equation was solved to obtain

(14) (a) Jepsen, O.; Burkhardt, A.; Andersen, O. K. *The Program TB-LMTO-ASA*, version 4.7; Max-Planck-Institut für Festkörperforschung: Stuttgart, Germany, 2000; (b) Blöchl, P. E.; Jepsen, O.; Andersen, O. K. *Phys. Rev. B* **1994**, *49*, 16223–16233.

Table 3. Selected Interatomic Distances (Å) in the Structures of Parameters for $LaRu_2Al_2B$, $La_2Ni_{1.79(1)}Ru_{0.21(1)}Al$ (II), $La_2Ni_{1.24(1)}Ru_{0.76(1)}Al$ (III), and $La_6SnNi_{3.67}Ru_{0.76}Al_{3.6}$ (IV)

$LaRu_2Al_2B$ (I)	distance, Å	$La_6SnNi_{3.67}Ru_{0.76}Al_{3.6}$ (IV)	distance, Å
La(1)−B(2)	2.8306(4) × 2	Al(7)/Ru(7)−Ni(3)	2.540(1) × 3
La(1)−Al(3)	3.2876(6) × 8	Ni(6)−Al(4)	2.673(2) × 6
La(1)−Ru(4)	3.5277(4) × 8	Ni(3)−Ni(6)	3.014(1)
B(2)−Ru(4)	2.1053(3) × 4	Al(4)−Ni(3)	2.561(1) × 2
Al(3)−Ru(4)	2.5486(7) × 4	Al(4)−Ni(6)	2.673(1) × 2
Al(3)−Al(3)	2.789(3)	Al(4)−Al(4)	2.779(4) × 2
Al(3)−Al(3)	2.873(3)	Sn(5)−La(2)	3.3885(5) × 6
Ru(4)−B(2)	2.1053(3) × 2	Sn(5)−La(1)	3.424(1) × 3
Ru(4)−Al(3)	2.5486(7) × 4	Ni(3)−Al(4)	2.562(1) × 2
Ru(4)−Ru(4)	2.9773(4) × 4		
$La_2Ni_{1.8}Ru_{0.2}Al$ (II)	distance, Å	$La_2Ni_{1.2}Ru_{0.8}Al$ (III)	distance, Å
Ni(2)/Ru(2)−Ni(2)/Ru(2)	2.658(2)	Ni(2)/Ru(2)−Ni(2)/Ru(2)	2.6593(7)
Ni(2)/Ru(2)−Ni(2)/Ru(2)	3.000(2)	Ni(2)/Ru(2)−Ni(2)/Ru(2)	3.0662(7)
Ni(2)/Ru(2)−Al(3)	2.596(2)	Ni(2)/Ru(2)−Al(3)	2.5793(4)
Ni(2)/Ru(2)−Al(3)	2.5969(8)	Ni(2)/Ru(2)−Al(3)	2.5929(7)

the partial waves. No empty spheres had to be added. The calculation was made for 819 κ points in the irreducible Brillouin zone. Integration over the Brillouin zone was made by the tetrahedron method.[14b] The following radii of atomic spheres were applied for the calculations: r(La) = 2.15 Å, r(Ru) = 1.33 Å, r(Al) = 1.59 Å, r(B) = 1.08 Å. The basis set contained La (6s, 5d, 4f), Ru (5s, 5p, 4d), Al (3s, 3p) and B (2s, 2p) with La(6p), Ru(4f), Al(3d), and B(3d) functions being downfolded. ELF,[15] η, was calculated on an adequately fine mesh of 0.03 Å. The Data Explorer program[16] was used for visualization of ELF isosurfaces. The topology of ELF was analyzed using the program Basin implemented into DGrid v.4.4.[17]

Results and Discussion

Our attempts to obtain ruthenium intermetallics from La−Ni flux led to the preparation of three new compounds $LaRu_2Al_2B$ (I), $La_2Ni_{2-x}Ru_xAl$ (II and III), and $La_6SnNi_{3.67}Ru_{0.76}Al_{3.6}$ (IV). Three types of crystals different by habit and color were selected from the reaction with initial composition La/Ru/Sn/B = 1:1:1:1 in an excess of La−Ni eutectic. The strongly reducing La−Ni flux leached Al from the crucible giving rise to aluminum incorporation into all three compounds; deliberate addition of Al in later reactions increased the yield of products. The structures of the new compounds were successfully determined from single crystal X-ray diffraction data. EDXS analysis of several crystals with defined unit cells confirmed the refined composition and absence of nickel in the case of $LaRu_2Al_2B$ and presence of ruthenium and nickel in the case of $La_2Ni_{1.8}Ru_{0.2}Al$ (II), $La_2Ni_{1.2}Ru_{0.8}Al$ (III), and $La_6SnNi_{3.67}Ru_{0.76}Al_{3.6}$ (IV).

Subsequently, relatively large single crystals (up to 1 mm) of $LaRu_2Al_2B$ were synthesized from La−Ni eutectic by adding a 1:2:2:1 stoichiometric mixture of La, Ru, Al, B. These crystals have a distinctive pink color and metallic luster and could be easily distinguished from the LaNiAl byproduct crystals (identified by single crystal XRD) formed in the sample. The crystals of $LaRu_2Al_2B$ are air-sensitive and degrade if left in air for a long period of time, but withstand overnight X-ray data collections under ambient conditions.

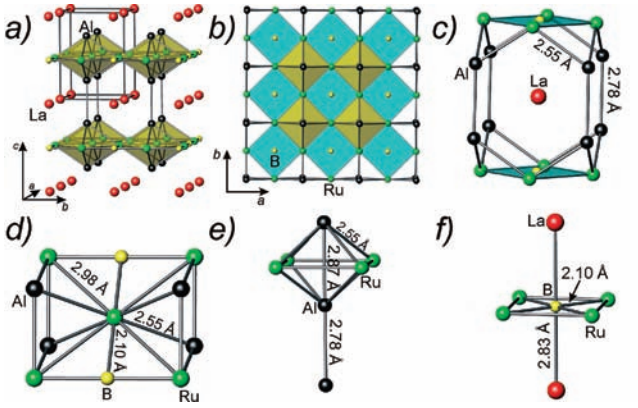

Figure 1. (a) Crystal structure of $LaRu_2Al_2B$. (b) Square net of Ru atoms with Ru_4Al_2-octahedra (yellow) and boron-centered Ru_4-squares (blue) emphasized. Local coordination of (c) La, (d) Ru, (e) Al, and (f) B.

Isolating the formation of the other phases (II, III, and IV) proved more difficult. Reactions of La/Ru/Al and La/Ru/Al/Sn in the La/Ni eutectic yield known La−Ni−Al ternary phases in addition to the desired products.

$LaRu_2Al_2B$. Crystal Structure. $LaRu_2Al_2B$ (Figure 1) has the tetragonal $CeCr_2Si_2C$ structure type,[18] which can be viewed as a "filled" or "stuffed" variant of the $CeMg_2Si_2$ structure.[19] Ruthenium atoms form a square net with boron atoms centering alternating squares, producing a flat [Ru_2B] layer. Aluminum atoms are situated above and below the remaining Ru-squares in such a way that distorted empty [Ru_4Al_2]-octahedra are formed. [Ru_2BAl_2] layers are stacked along the c-axis with an Al−Al interlayer distance of 2.79 Å. Thus, aluminum is coordinated by four Ru atoms at a distance of 2.55 Å, one aluminum atom from another layer at a distance of 2.79 Å, and also has a contact of 2.87 Å with aluminum from the same layer, situated across the Ru−B net.

Ruthenium is coordinated by four ruthenium atoms at a distance of 2.98 Å, two boron atoms at a distance of

(15) (a) Becke, A. D.; Edgecombe, K. E. *J. Chem. Phys.* **1990**, *92*, 5397–5403. (b) Savin, A.; Jepsen, O.; Flad, J.; Andersen, O. K.; Preuss, H.; von Schnering, H. G. *Angew. Chem., Int. Ed. Engl.* **1992**, *31*, 187–188.

(16) *IBM's Open Visualization Data Explorer*, Version 4.4.4; http://www.opendx.org.

(17) Kohout, M. *DGrid*, version 4.4; Radebeul, Germany, 2008.

(18) (a) Tang, C.; Fan, S.; Zhu, M. *J. Alloys Compd.* **2000**, *299*, 1–4. (b) Pohlkamp, M. W.; Jeitschko, W. *Z. Naturforsch.* **2001**, *B56*, 1143–1148. (c) Klosek, V.; Vernière, A.; Malaman, B.; Tobola, J.; Kaprzyk, S. *Phys. Rev B* **2008**, *78*, 104419. (d) Janatova, M.; Vejpravova, J.; Divis, M.; Sechovsky, V. *Physica B* **2008**, *403*, 2338–2343.

(19) Zmii, O. F.; Gladyshevskij, E. I. *Sov. Phys. Crystallogr.* **1971**, *15*, 871.

2.10 Å in the *ab*-plane, and by four aluminum sites at a distance of 2.55 Å in the *ac*-plane. The Ru−Ru distance of 2.98 Å is longer than that in ruthenium metal (2.68−2.72 Å), but is comparable with typical Ru−Ru distances ranging from 2.78−3.05 Å found in La−Ru compounds with $ThCr_2Si_2$ structure type ($LaRu_2Si_2$[20] and $LaRu_2Ge_2$[21]), in ternary borides of ruthenium and aluminum $Ru_3Al_2B_2$ and $Ru_4Al_3B_2$,[22] and in ternary borides of La and Ru ($LaRu_3B_2$[23] and $La_3Ru_8B_6$[24]).

Boron is found in the center of perfect Ru_4-squares with a Ru−B distance of 2.10 Å. Square planar coordination of boron by transition metals is rather unusual; boron-centered transition metal trigonal prisms or octahedra are far more common coordination polyhedra in borides with low boron content (M/B > 4). To the best of our knowledge, the borides Ga_8Ir_4B[25] and $Y_2Pd_{14}B_5$[26] are the only two examples of boron with square planar coordination. In the structure of Ga_8Ir_4B boron centers almost perfect Ir_4-squares at a distance of 2.13 Å and 2.15 Å, while in $Y_2Pd_{14}B_5$ one boron position has a square planar coordination of four Pd at a distance of 2.54 Å. The Ru−B distance of 2.10 Å in $LaRu_2Al_2B$ is shorter than the Ir−B distance in Ga_8Ir_4B (in agreement with the smaller metallic radius of ruthenium compared to iridium) and is within the 2.05−2.26 Å range of Ru−B distances in ternary Ru borides $CeRu_2B_2$,[27] $LaRu_3B_2$,[23] $La_3Ru_8B_6$[24] and $Sr_2Ru_7B_8$.[28] Each boron atom also has two long and predominantly ionic (vide infra) La−B contacts of 2.83 Å along the *c*-axis, within the 2.71−2.99 Å range of La−B distances found in borides $LaCo_2B_2$,[29] $LaRu_4B_4$[30] and lanthanum-rich borocarbides LaB_2C_2 and LaBC.[31] Each La cation is found in the center of a 16-vertex cage composed of 8 ruthenium and 8 aluminum atoms with boron atoms sited directly above and below the lanthanum site along the *c*-axis.

The $CeMg_2Si_2$ structure is closely related to the $ThCr_2Si_2$ structure type observed for a vast number of intermetallic compounds. In the structure of $ThCr_2Si_2$ each Cr_4-square has only one apical Si atom; these are situated below and above the chromium layer in a staggered order, whereas in the $CeMg_2Si_2$ structure silicon atoms are found above and below the same Mg_4-square. Silicides $LnCr_2Si_2$ (Ln = Y, Nd, Sm, Gd−Lu) crystallize in the $ThCr_2Si_2$-type. Addition of carbon leads to the stabilization of the filled $CeMg_2Si_2$-type structure found for $LnCr_2Si_2C$ (Ln = Y, La−Nd, Sm, Gd−Er).[18] Many

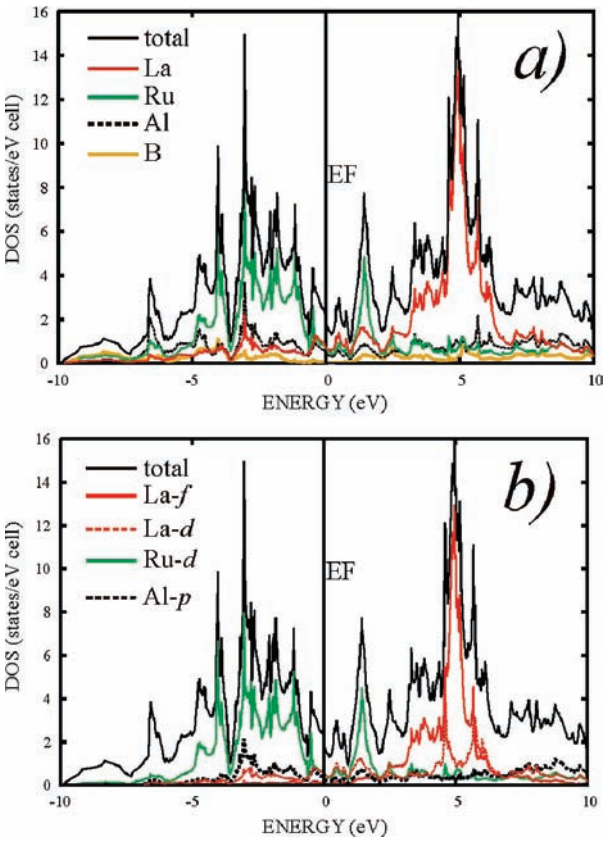

Figure 2. Total and partial density of states for $LaRu_2Al_2B$. (a) contributions from La, Ru, Al, B and (b) La-f, La-d, Ru-d, Al-p states are color-coded.

ruthenium intermetallics $LnRu_2X_2$ (Ln is rare-earth metal, X = Ge or Si, P or As) have the $ThCr_2Si_2$ structure type; however aluminides "$LnRu_2Al_2$" or borides "$LnRu_2B_2$" with the $ThCr_2Si_2$ structure are not known. The addition of boron leads to the stabilization of the filled $CeMg_2Si_2$ structure type, thus to the formation of $LaRu_2Al_2B$ compound. Another factor which may play a substantial role in stabilizing $LaRu_2Al_2B$ with the filled $CeMg_2Si_2$-type is valence electron count (VEC). VEC for the $[Cr_2Si_2C]^{3-}$ anionic moiety is equal to 27, taking into account the +3 oxidation state of the rare-earth metals Ln and *d*-electrons of Cr. The VEC of 28 for the $[Ru_2Al_2B]^{3-}$ anionic unit is very close to that of $[Cr_2Si_2C]^{3-}$, while the VEC of 31 for hypothetical "$[Ru_2Si_2C]^{3-}$" is considerably larger. Apparently, the larger of number of *d*-electrons of Ru compared to Cr is compensated by substitution of silicon and carbon for aluminum and boron, respectively, keeping a VEC of around 27 and stabilizing the $LnCr_2Si_2C$ structure type. Band structure and ELF calculations were performed to further investigate the electronic structure of $LaRu_2Al_2B$.

Electronic Structure and Chemical Bonding. Total and partial density of states (DOS) diagrams are presented in Figure 2. $LaRu_2Al_2B$ is found to be metallic with the Fermi level residing close to a pseudo-gap and $N(E_F)$ = 2.8 states eV^{-1} per unit cell at E_F. The states between −10 eV and the Fermi level are composed of mainly Ru, La, and Al basis functions. The boron contribution to the states near E_F is much smaller, the boron states have high dispersion, indicating strong hybridization with those of Ru, La, and Al. Aluminum states are mainly of *p*-char-

(20) Hiebl, K.; Horvath, C.; Rogl, P.; Sienko, M. *J. Magn. Magn. Mater.* **1983**, *37*, 287–296.
(21) Francois, M.; Venturini, G.; Mareche, J. F.; Malaman, B.; Roques, B. *J. Less-Common Met.* **1985**, *113*, 231–237.
(22) Jung, W.; Schweitzer, K. *Z. Kristallogr.* **1986**, *174*, 109–110.
(23) Ku, H. C.; Meisner, G. P.; Acker, F.; Johnston, D. C. *Solid State Commun.* **1980**, *35*, 91–96.
(24) Sologub, O. L.; Salamakha, L. P.; Noël, H.; Roisnel, T.; Gonçalves, A. P. *J. Solid State Chem.* **2007**, *180*, 2740–2746.
(25) Klünter, W.; Jung, W. *Z. Angew. Allg. Chem.* **1995**, *621*, 197–200.
(26) Salamakha, P.; Gonçalves, A. P.; Sologub, O. L.; Almeida, M. *J. Alloy Cmpd.* **2003**, *360*, 61–68.
(27) Horvath, C.; Rogl, P.; Hiebl, K. *J. Solid State Chem.* **1987**, *67*, 70–77.
(28) Jung, W.; Diessenbacher, F. *Z. Angew. Allg. Chem* **1991**, *594*, 57–65.
(29) Niihara, K.; Shishido, T.; Seishi, Y. *Bull. Chem. Soc. Jpn.* **1973**, *46*, 1137–1140.
(30) Grüttner, A.; Yvon, K. *Acta Crystallogr.* **1979**, *B35*, 451–453.
(31) (a) Bauer, J.; Bars, O. *Acta Crystallogr.* **1980**, *B36*, 1540–1544. (b) Babizhetskyy, V.; Mattausch, H.; Gautier, R.; Bauer, J.; Halet, J. F.; Simon, A. *Z. Angew. Allg. Chem* **2005**, *631*, 1041–1046.

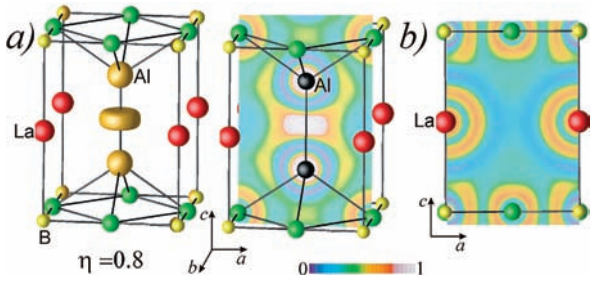

Figure 3. (a) 3-D isosurfaces of electron localization function (η) at η = 0.8 and 2-D coloring of the η distribution showing the Al−Al covalent bond; color bar is shown below. (b) Slice of the structure of $LaRu_2Al_2B$ along the *c*-axis showing the closed-shell ELF-distribution around La atoms.

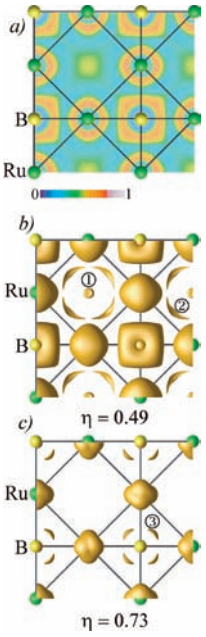

Figure 4. (a) Coloring of the electron localization function (η) distribution for the [Ru_2B] layer in the crystal structure of $LaRu_2Al_2B$ (color bar, below). (b) 3-D isosurface of the electron localization function for η = 0.49 for the [Ru_2B] layer. Localization domain ① corresponds to 2c-bond between two Al atoms capping the same Ru_4-square, ② represents four three-center bonds between the Al atom and sets of two adjacent Ru atoms from the square net. (c) 3-D isosurface of the ELF for η = 0.73 for the [Ru_2B] layer. Domain ③ indicates four three-center bonds between the central B and sets of two adjacent Ru atoms.

acter. The contribution of Ru is mainly from the *d*-band, which is not completely filled, since there is a large Ru peak at about 2 eV above E_F. The empty lanthanum 4*f* band is located about 5 eV above Fermi level, while La-*d* orbitals contribute to states closer to E_F.

The chemical bonding was analyzed using the electron localization function (ELF). The localization domain located in the center of the Al−Al distance of 2.79 Å corresponds to a covalent Al−Al bond (Figure 3a). The spatial distribution of ELF near La atoms has a pronounced shell-like character; this indicates that La behaves as a closed-shell cation La^{3+}, and the interactions between La and surrounding atoms are predominantly ionic (Figure 3b). The bonding within the [Ru_4B]-layer is more complex (Figure 4). The basin (not shown) of the localization domain ① in the center of the Ru_4Al_2-octahedron (Figure 4a) has common surfaces only with the core basins of the two Al atoms, corresponding to two-center covalent bonding between two aluminum atoms capping the same Ru_4-square with an Al−Al distance of 2.87 Å. The aluminum atoms therefore form a chain running parallel to the *c*-axis, consisting of covalent Al−Al bonds alternating in length.

The localization domain ② (Figure 4b) corresponds to four multicenter bonding interactions, each of which involves a three-center bond between aluminum and two adjacent ruthenium atoms from the square net. Thus, each aluminum atom is involved in covalent bonding with two neighboring Al atoms, and also participates in four three-center bonding interactions with Ru atoms. A similar situation is seen for boron, with localization domain ③ (Figure 4c) revealing three-center bonds between the central B atom and two adjacent ruthenium atoms; each boron atom centering a Ru_4-square is involved in four interactions of this type. It is notable that no attractors were found between ruthenium atoms, that is, on the sides of the Ru_4-squares. Therefore, this [Ru_2B]-layer is best described not as a square net of bonded Ru atoms centered by boron atoms, but instead as linked [Al_2Ru_4] octahedra and [Ru_4B] planar units.

The dimensionality and the nature of the bonding in several metal borides have been studied by analysis of distribution of ELF-attractors and shown to be dependent on the metal to boron (M/B) ratio.[32] For instance, in borides with high boron content such as $Mg_2Rh_{1-x}B_{6+2x}$ (low M/B∼0.5), the ELF maxima are found between B−B contacts, corresponding to 2*c*-2*e* covalent bonding in a three-dimensional (3-D) boron polyanion.[32b] A higher M/B ratio is found in $Mg_{1-x}RhB$ (M/B ∼ 2); in this structure, rhodium and boron form a two-dimensional (2-D) polyanion, which acts as a counteranion for Mg^{2+}.[32c] An even higher metal to boron ratio (M/B = 12) in Mg_8Rh_4B leads to reducing of the dimensionality of the anionic part to 0-D isolated [Rh_4B] clusters; bonding analysis using ELF reveals maxima located on the four Rh−B bonds, which correspond to 2*c*-2*e* covalent interactions.[32a] In $LaRu_2Al_2B$ (M/B = 5), the different geometrical arrangement of transition metals around boron together with smaller number of valence electrons of ruthenium compared with rhodium leads to a very different type of boron bonding. Multicenter Ru−B and Ru−Al bonding is realized within the [Ru_2Al_2B] layer, but these layers are connected by covalent 2*c*-2*e* Al−Al bonds. Therefore the structure of $LaRu_2Al_2B$ should be viewed as a 3-D polyanion [Ru_2Al_2B] with charge-balancing La^{3+} cations rather than as a 2-D layered structure.

Magnetic Properties and Specific Heat. The magnetic susceptibility of the $LaRu_2Al_2B$ phase measured with an applied field of 3000 Oe is positive and nearly temperature-independent (Figure 5). Temperature-independent paramagnetism (TIP) is typically due to conduction electrons, indicating this compound behaves as a Pauli paramagnet. A plot of χT versus T yields a line which intersects

(32) (a) Alekseeva, A. M.; Abakumov, A. M.; Leithe-Jasper, A.; Schnelle, W.; Prots, Y.; Chizhov, P. S.; Van Tendeloo, G.; Antipov, E. V.; Grin, Y. *J. Solid State Chem.* **2006**, *179*, 2751–2760. (b) Alekseeva, A. M.; Abakumov, A. M.; Chizhov, P. S.; Leithe-Jasper, A.; Schnelle, W.; Prots, Yu.; Hadermann, J.; Antipov, E. V.; Grin, Yu. *Inorg. Chem.* **2007**, *46*, 7378–7386. (c) Alekseeva, A. M.; Abakumov, A. M.; Leithe-Jasper, A.; Schnelle, W.; Prots, Yu.; Hadermann, J.; Van Tendeloo, G.; Antipov, E. V.; Grin, Yu. *Z. Angew. Allg. Chem.* **2005**, *631*, 1047–1054.

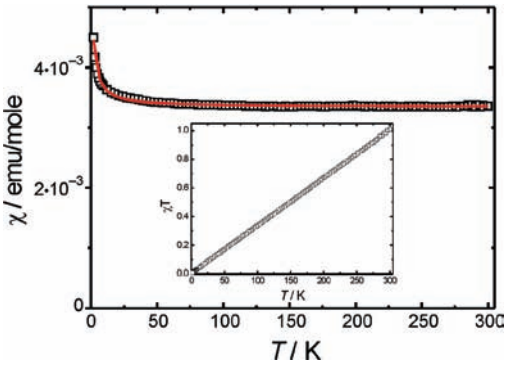

Figure 5. Temperature dependence of magnetic susceptibility for $LaRu_2Al_2B$, $\chi(T)$ at an applied field of 3000 Oe. Inset: χT versus T.

both axes at 0 K (Figure 5, inset), also indicative of Pauli paramagnetism and typical for metallic conductors. This is in agreement with the calculated DOS, which predicts metallic behavior. The susceptibility data was fitted with a modified Curie−Weiss law: $\chi = \chi_{TIP} + C/(T - \theta) = (3.340(1) \times 10^{-3}) + [(3.68(8) \times 10^{-3})/(T + 1.5(9))]$. The value of χ_{TIP} of $3.340(1) \times 10^{-3}$ emu/mol is somewhat large, possibly stemming from paramagnetic impurities. Susceptibility data collected at applied fields below 1000 Oe (Supporting Information, Figure S1) revealed traces of superconductivity with $T_c \leq 6$ K. This indicates the presence of a residual surface film or occlusions of β-La, which becomes superconducting at $T_c \approx 6$ K ($H_c = 1000$ Oe).[33]

To further investigate the electronic properties of $LaRu_2Al_2B$ the temperature dependence of specific heat was measured (Figure 6). The specific heat of a solid is the sum of electron (C_e) and lattice (C_l) contributions. For $LaRu_2Al_2B$, the lattice contribution, C_l, is large compared to C_e, and at low temperatures it requires three terms in the harmonic-lattice approximation for an adequate fit: $C_l = \beta T^3 + \beta_1 T^5$. In the normal state, C_e is expected to be of the form $C_e = \gamma T$, where γ is the Sommerfeld coefficient, proportional to the total DOS at the Fermi level $N(E_F)$: $\gamma = {}^1/_3\pi^2 k_B{}^2 N(E_F)$. The fit to the theoretical equation is shown in Figure 6 (red line), yielding the parameters $\gamma = 7.05$ mJ/mol·K^2, $\beta = 0.2$ mJ/mol·K^4 and $\beta_1 = 7.1 \times 10^{-4}$ mJ/mol·K^6. The value of γ corresponds to a total DOS at the Fermi level of $N(E_F) = 3.0$ states/eV·unit cell. This agrees well with the value of $N(E_F)$ derived from DOS calculations (2.8 states eV^{-1} per cell), both indicating metallic behavior of $LaRu_2Al_2B$. The coefficient β is related to the Debye temperature (θ_D) as $\beta = 12/5\pi^4 Rn(\theta_D)^{-3}$, where R is the gas constant and n is the number of atoms per formula unit. The Debye temperature for $LaRu_2Al_2B$ was found to be $\theta_D = 329$ K. This Debye temperature, which is a measure of lattice stiffness, is comparable with values of 271 and 299 K for Ru-based $ThCr_2Si_2$-type compounds $BaRu_2As_2$ and $LaRu_2Si_2$.[34,35] The deviations of C_l from the T^3 term (the differences between the red and the blue line in Figure 6) indicate a strong effect of phonon dispersion.

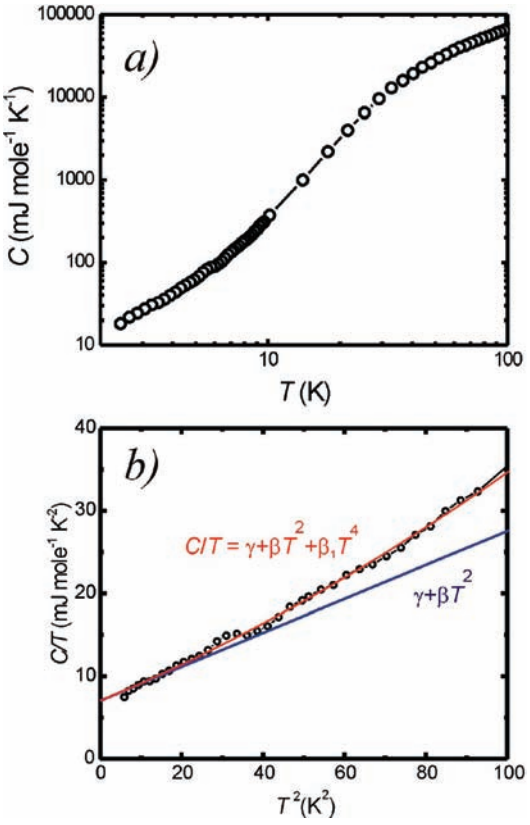

Figure 6. (a) Temperature dependence of specific heat, $C_p(T)$ of $LaRu_2Al_2B$ from 2 to 100 K in zero magnetic field. (b) C/T versus T^2 plot and its linearization (see text for details).

$La_2Ni_{2-x}Ru_xAl$ ($x = 0.21(2)$ and $0.76(1)$). The monoclinic structure of $La_2Ni_{2-x}Ru_xAl$ (Figure 7a and b) features infinite $[AlNi_{2-x}Ru_x]$-spiral-twisted chains running along the *c*-axis. The chains are composed of nearly flat $Al_2Ni_{2-x}Ru_x$-rhombic units connected by corner-sharing aluminum atoms and twisted at ~70° relative to each other (Figure 7b), producing highly distorted tetrahedral coordination of the aluminum atoms by Ni/Ru. The chains are not isolated from each other; they are linked by Ni(Ru)−Ni(Ru) bonds (2.66 Å) in the *ab*-plane forming a 3-D structure with channels in which La^{3+} cations reside. Each Ni/Ru atom is coordinated by two Al atoms at a distance of 2.60 Å and one Ni/Ru atom at a distance of 2.66 Å. Two analogues of this structure were characterized, with different Ni/Ru ratios; increasing the amount of Ru on the 8*f* site results in an expansion of the unit cell. It is likely that the Ni/Ru ratio could be varied using different ratios of starting reagents, but precise determination of the phase width is hampered because of the nickel-rich environment of the flux.

Seven compounds were reported to crystallize with the same structure type as $La_2Ni_{2-x}Ru_xAl$: Gd_2Ge_2Al (VEC = 17),[36] Ca_2Ir_2Si (VEC = 26),[37] HT-Pr_2Co_2Al (VEC = 27),[38]

(33) (a) Ziegler, W. T.; Young, R. A.; Floyd., A. L., Jr. *J. Am. Chem. Soc.* **1953**, *75*(5), 1215–1221. (b) Roberts, B. W. *J. Phys. Chem. Ref. Data* **1976**, *5*, 591–821.
(34) Nath, R.; Singh, Y.; Johnston, D. C. *Phys. Rev. B* **2009**, *79*, 174513.
(35) Gondek, L.; Szytuła, A.; Slaski M. *Solid State Commun.* **2006**, *140*, (2006) 141−143.
(36) Choe, W.; McWhorter, S.; Miller, G. J. *Z. Anorg. Allg. Chem.* **2002**, *628*, 1575–1580.
(37) Schoolaert, S.; Jung, W. *Z. Anorg. Allg. Chem.* **2002**, *628*, 1806–1810.
(38) Pani, M.; Merlo, F.; Fornasini, M. L. *Z. Kristallogr.* **2002**, *217*, 415–419.

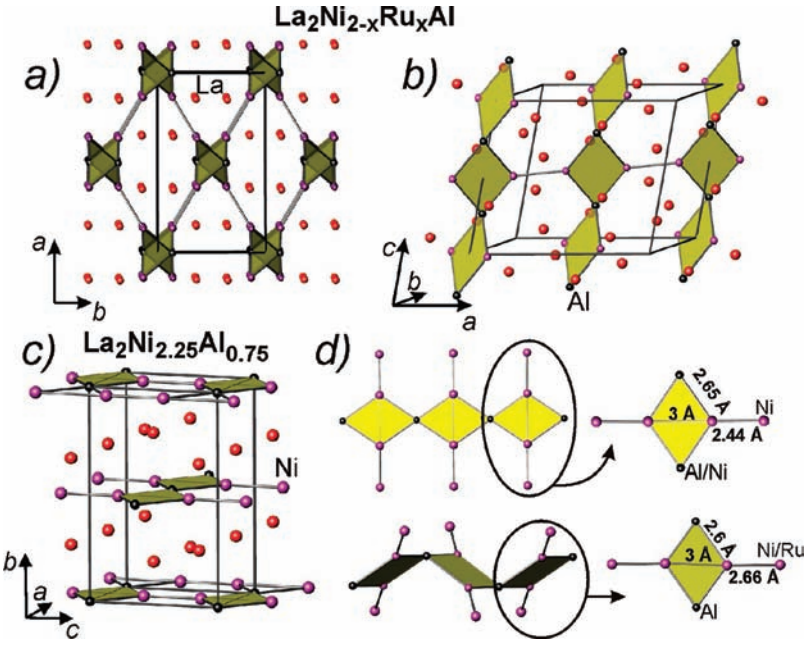

Figure 7. Crystal structure of $La_2Ni_{2-x}Ru_xAl$ in (a) projection on *ab*-plane and (b) viewed down *b*-axis; (c) the crystal structure of $La_2Ni_{2.25}Al_{0.75}$;[40] (d) structural motif and the common rhombic units found in the crystal structures of $La_2Ni_{2.25}Al_{0.75}$ (top) and $La_2Ni_{2-x}Ru_xAl$ (bottom).

and R_2M_2In (R = Ca, Sr; M = Pd, Pt; VEC = 27).[39] The first analogue is the only example that does not contain a transition metal. The narrow range of VEC values for the analogues containing transition metals may indicate the importance of Ru incorporation in stabilizing this structure type. The VEC number for $La_2Ni_{2-x}Ru_xAl$ (VEC = 28.6 for $x = 0.21$ and VEC = 27.5 for $x = 0.76$) is very close to that for HT-Pr_2Co_2Al-type phases containing *d*-metals. One can assume that the hypothetical isostructural La_2Ru_2Al compound is not stable because of the relatively low VEC of 25. A La_2Ni_2Al analogue is also not known; this would have a VEC of 29. The absence of Ru and resulting high VEC promotes crystallization of a closely related phase instead, namely, orthorhombic $La_2Ni_{2.25}Al_{0.75}$ (Mo_2NiB_2-type, Figure 7c).[40] Although the compositions of both compounds can be denoted as $La_2(M/Al)_3$ (M = Ni or Ru/Ni), and both feature chains of vertex-sharing $[Al_{2-x}M_{2+x}]$-rhombic units which are interlinked by Ni−Ni bonds, their crystal structures are different. In the crystal structure of $La_2Ni_{2.25}Al_{0.75}$ the derived layers are flat with a Ni−Ni distance of 2.44 Å, while in the structure of $La_2Ni_{2-x}Ru_xAl$ the interchain Ni(Ru)−Ni(Ru) distance is longer (2.66 Å), which is in line with larger atomic radius of Ru compared to Ni (r(Ni) = 1.15 Å, r(Ru) = 1.25 Å) (Figure 7d). Thus, the $La_2Ni_{2-x}Ru_xAl$ phase can be viewed as a new lanthanum−nickel aluminide stabilized by ruthenium, which is compositionally and structurally related to the ternary $La_2Ni_{2.25}Al_{0.75}$ phase.

Ten phases are reported in the ternary La−Ni−Al system (Supporting Information, Table S2). The flat $[Al_2Ni_2]$-rhombic unit serves as a building block in all the structures in which Ni and Al occupy unique sites (not mixing on identical sites as seen for $LaNi_{13-x}Al_x$[41] and $LaNi_{5-x}Al_x$[42]) and with Ni/Al ratio larger than 0.14 (all except La_2Al_7Ni[43]). The crystal structures of these phases follow the trend of decreasing dimensionality of the Ni/Al anionic moiety (from framework to layer to chain) with increasing of La content. At low La content the $[Al_2Ni_2]$-rhombic units have a relatively long non-bonding Ni−Ni (∼ 4 Å) distance within the rhombs, and these $[Al_2Ni_2]$-units share edges and vertices to form a 3-D Ni/Al framework (seen in phases $LaAl_5Ni_2$,[44] $LaNi_{1+x}Al_{6-x}$,[45] $LaNi_2Al_3$,[46] and LaNiAl[47]). In the structure of $LaNiAl_2$[48] a corrugated layer is formed from vertex- and edge-sharing $[Al_2Ni_2]$-rhombic units, each having a non-bonding Ni−Ni distance (∼4 Å) within the rhombs. With further increase of La content (crystal structure of $La_2Ni_{2.25}Al_{0.75}$[40]) the Ni−Ni distance within the $[Al_{2-\delta}Ni_{2+\delta}]$-rhombic unit becomes shorter (3 Å), and the $[Al_{2-\delta}Ni_{2+\delta}]$-rhombic units share vertices to form a flat layer. $La_5Ni_2Al_3$[49] is the phase with the largest lanthanum content; in its crystal structure $[Al_2Ni_2]$ rhombs are isolated from each other and feature a bonding Ni−Ni distance of 2.68 Å. Thus, the increase of

(39) (a) Muts, I. R.; Zaremba, V. I.; Rodewald, Wilfried, U. Ch.; Hermes, W.; Pöttgen, R. *Z. Anorg. Allg. Chem.* **2007**, *633*, 2725–2729. (b) Muts, I.; Nilges, T.; Rodewald, U. Ch.; Zaremba, V. I.; Pöttgen, R. *Z. Naturforsch.* **2007**, *62b*, 1563–1566.
(40) Romaka, V. A.; Grin', Yu. N.; Yarmolyuk, Ya. P.; Zarechnyuk, O. S.; Skolozdra, R. V. *Fiz. Metal. Metalloved.* **1982**, *54*, 691–696.
(41) Gladyshevsky, E. I.; Bodak, O. I.; Pecharsky, V. K. In *Handbook of the Physics and Chemistry of Rare Earths*; Gschneider, K. A., Jr., Eyring, L., Eds.; North-Holland : Amsterdam, 1990; Vol. *13*.
(42) Diaz, H.; Percheron-Guégan, A.; Achard, J. C.; Chatillon, C.; Mathieu, J. C. *Int. J. Hydrogen Energy* **1979**, *4*, 445–454.
(43) Gout, D.; Barker, T. J.; Gourdon, O.; Miller, G. J. *Chem. Mater.* **2005**, *17*, 3661–3667.
(44) Yarmolyuk, Ya.P.; Rykhal, R. M.; Aksel'rud, L. G.; Zarechnyuk, O. S. *Dopov. Akad. Nauk. Ukr. RSR. Seriya A* **1981**, *A 9*, 86–90.
(45) Gout, D.; Benbow, E.; Gourdon, O.; Miller, G. J. *Inorg. Chem.* **2004**, *43*, 4604–4609.
(46) Gladyshevskii, R. E.; Cenzual, K.; Parthé, E. *Acta Crystallogr.* **1992**, *B48*, 389–392.
(47) Cordier, G.; Dörsam, G.; Kniep, R. *J. Magn. Magn. Mater.* **1988**, *76−77*, 653–654.
(48) Bruzzone, G.; Ferretti, M.; Merlo, F.; Olcese, G. L. *Lanthanide Actinide Res.* **1986**, *1*, 153–161.
(49) Leineweber, A.; Nitsche, H. *Z. Anorg. Allg. Chem.* **2006**, *632*, 553–558.

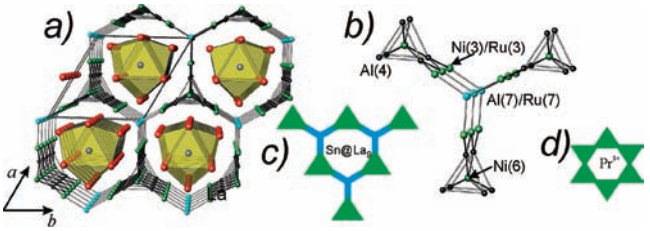

Figure 8. (a) Crystal structure of $La_6SnNi_{3.67}Ru_{0.76}Al_{3.6}$ viewed down the *c*-axis. Coordination polyhedra of Sn by La atoms are drawn in yellow; La is represented by red spheres, Sn atoms by gray, Ni or Ni/Ru by green, Al by black, and mixed Ru/Al sites by cyan spheres. (b) The local coordination environment of the Ru, Al and Ni atoms. (c) and (d) Models of the Ni/Ru/Al and Ni/Al networks found in the structures of $La_6SnNi_{3.67}Ru_{0.76}Al_{3.6}$ and $PrNi_2Al_3$, respectively (green triangles, Al_6 trigonal prism centered by Ni or Ni/Ru atoms; blue connecting units, trigonal-planar MNi_3 units, M = Al/Ru).

lanthanum content within ternary La−Ni−Al phases not only changes the dimensionality of the anionic Ni/Al building block, but also leads to a change in the Ni−Ni interaction within the $[Al_2Ni_2]$-rhombs from non-bonding to bonding.

$La_6SnNi_{3.67}Ru_{0.76}Al_{3.6}$. The structure of $La_6SnNi_{3.67}Ru_{0.76}Al_{3.6}$ can be viewed as a hexagonal Ni/Ru/Al framework with large channels hosting tin-centered lanthanum clusters Sn@La_9 (@ = encapsulated) (Figure 8, Table 3). The framework is composed of Ni, Al, and Ru atoms with 1*a* and 3*j* sites occupied by Ru/Al and Ru/Ni, respectively. Although the role of ruthenium in the stabilization of $La_6SnNi_{3.67}Ru_{0.76}Al_{3.6}$ crystal structure is not clear, its presence is required; this phase is not formed in reactions without ruthenium. The Al/Ru site forms trigonal planar units with three Ni(3)/Ru(3) atoms with a bond distance of 2.54 Å. Three Ni(3)/Ru(3) atoms in turn are connected by sharing two Al atoms (d(Ni/Ru−Al) = 2.56 Å) with trigonal prisms of aluminum which are centered by Ni(6) atoms featuring Ni−Al distances of 2.67 Å (Figure 8b, Table 3). The extension of these interconnected units leads to a 3-D framework with large hexagonal channels (Figure 8c). Tin atoms are coordinated by nine La atoms (Figure 8a), which form a tricapped trigonal prism around tin with La−Sn distances of 3.39 Å and 3.42 Å, comparable to La−Sn distances of 3.33 Å−3.66 Å in binary La_5Sn_3[50] (W_5Si_3-type). In the structure of $La_6SnNi_{3.67}Ru_{0.76}Al_{3.6}$ the tricapped trigonal prism Sn@La_9 clusters are connected by sharing two trigonal faces forming Sn@La_6 (or Sn@$La_3La_{6/2}$) columns running along the *c*-axis and filling the large hexagonal channels.

The hexagonal channels found in the structure of $La_6SnNi_{3.67}Ru_{0.76}Al_{3.6}$ are related to those found in the crystal structure of $PrNi_2Al_3$[51] (ordered variant of $CaCu_5$-type) (Figure 8d). In the structure of $PrNi_2Al_3$ nickel atoms have the same trigonal prismatic coordination of six aluminum atoms. The Ni@Al_6 trigonal prisms are connected by sharing vertices, forming hexagonal channels in which Pr^{3+} cations reside (Figure 8d). In $La_6SnNi_{3.67}Ru_{0.76}Al_{3.6}$ similar Ni@Al_6 trigonal prisms are separated from each other and linked by trigonal-planar MNi_3 units (M = Al/Ru). This results in a greatly expanded hexagonal channel with a 10 Å diameter which can accommodate a larger counterion (Figure 8a and c). In the crystal structure of $La_6SnNi_{3.67}Ru_{0.76}Al_{3.6}$ the charge-balancing cations are not individual La^{3+} cations but are instead interconnected Sn@La_9 clusters. Assuming that the isolated central Sn atom has a −4 charge, the formal charge of the complex cationic chain [Sn@La_6] could be regarded as +14. The same structure motif is found for $Nd_6Co_5Ge_{2.2}$, with La and Sn positions occupied by Nd and Ge.[52] The positions within the hexagonal framework are occupied by Co, except for the 3*k* site, which is partially occupied by Ge. In the crystal structure of $La_6SnNi_{3.67}Ru_{0.76}Al_{3.6}$ this position is solely occupied by Al, while positions 1*a* and 3*j* feature mixed occupation by Al/Ru and Ni/Ru, respectively.

Conclusions

We have demonstrated that lanthanum/nickel flux is an excellent solvent for reactants ranging from boron and aluminum to ruthenium and tin. It is notable that both components of the flux were incorporated into several of the products isolated in this work. This is in contrast to reactions of iron in La/Ni flux, which often produce La/Fe/X intermetallics containing no nickel. The La/Ni eutectic flux offers a unique synthesis environment for growth of new, complex intermetallic phases. The similarity of binary phase diagrams of the early rare-earths and late transition metals to that of La−Ni indicates many other Ln-TM eutectics may be promising solvents for synthesis of new intermetallic compounds containing *f*-elements with interesting physical properties, for example, itinerant magnetism, spin glass behavior, heavy fermion behavior, and/or superconductivity.

Acknowledgment. The Authors thank Dr. A. Baranov (Max-Planck Institute for Chemical Physics of Solids, Dresden) and Dr. K. Kovnir (Chem. Dept., Florida State University) for fruitful discussion. We are indebted to Prof. David C. Larbalestier (Applied Superconductivity Center, NHMFL) for the opportunity to use PPMS. This research made use of the Scanning Electron Microscope facilities of MARTECH at Florida State University. Financial support from the NSF (Grant DMR-05-47791) is gratefully acknowledged.

Supporting Information Available: Crystallographic data for (I), (II), (III), and (IV) in the form of CIF files. Table S1 with interatomic distances in the structures of (I), (II), (III), (IV), Table S2 summarizing information about ternary La−Ni−Al phases, and Table S3 with results of EDX analysis. Figure S1 with plots of χ versus T at different external fields for $LaRu_2Al_2B$. This material is available free of charge via the Internet at http://pubs.acs.org.

(50) Kwon, Y. U.; Rzeznik, M. A.; Guloy, A.; Corbett, J. D. *Chem. Mater.* **1990**, *2*, 546–550.
(51) Rykhal', R. M.; Zarechnyuk, O. S.; Kuten', Ya. I. *Dopov. Akad. Nauk Ukr. RSR, Seriya A* **1978**, *12*, 1136–1138.
(52) Salamakha, P. S.; Pecharsky, V. K.; Bruskov, V. A.; Bodak, O. I. *Kristallografiya* **1986**, *31*, 587–589.